Scientific Experiences in Mechanical Engineering
Bridging Scientific Discovery and Technological Readiness in Mechanical Engineering
ISSN: 3164-3353
https://doi.org/10.68252/seme.6
Vol. 1, No. 1 (2027), pp. e6.1-13
Research Article

Thermo-Hydraulic Characteristics of TiO_2-SiO_2 Hybrid Nanofluids Utilizing Wire Coil Inserts: A Numerical Study

Anwar Ilmar Ramadhan[1]*, Wan Hamzah Azmi[2], Irnie Azlin Zakaria[3], Efrizon Umar[4]

[1] Department of Mechanical Engineering, Universitas Muhammadiyah Jakarta, Jl. Cempaka Putih Tengah 27 Jakarta, 10510 Indonesia
[2] Faculty of Mechanical and Automotive Engineering Technology, Universiti Malaysia Pahang Al-Sultan Abdullah, Pekan 26600, Pahang, Malaysia
[3] School of Mechanical Engineering, College of Engineering, Universiti Teknologi MARA (UiTM), 40450 Shah Alam, Selangor, Malaysia
[4] National Research and Innovation Agency, Jl. Tamansari No 71 Bandung, 40132, Indonesia

*Corresponding author: anwar.ilmar@umj.ac.id

Article History: Received: 29 June 2026 | Revised: 14 September 2026 | Accepted: 15 September 2026 | Published online: 16 September 2026

Abstract
The enhancement of heat transfer device performance through the use of wire coil inserts and hybrid nanofluids can significantly improve convective heat transfer, though it also results in higher pumping power requirements. Therefore, a comprehensive investigation considering both heat transfer improvement and the effects of friction factor and pressure drop on pumping power is essential. In this study, the heat transfer characteristics of TiO_2-SiO_2 hybrid nanofluids dispersed in an EG/water mixture within tubes equipped with wire coil inserts under constant wall heat flux were analyzed using computational fluid dynamics (CFD). Simulations were conducted with TiO_2-SiO_2 nanofluids at volume concentrations of 1.0, 2.0, and 3.0%, combined with wire coil inserts of varying pitch-to-diameter (P/D) ratios ranging from 0.2 to 0.8. Results show that the friction factor at 1.0% volume concentration increases with decreasing P/D ratio and Reynolds number, while the Nusselt number rises at a lower pitch ratio of 0.2. Furthermore, the thermal performance factor (TPF) was observed to increase as the pitch ratio decreased, with a maximum value of 1.43 at a P/D ratio of 0.2 for the 1.0% volume concentration.

Keywords: Experimental, Heat transfer, Hybrid nanofluids, Numerical, Wire coil

The Technology Readiness Level (TRL) of this research is Level 4 (Technology Validated in Laboratory). This study validated the thermo-hydraulic performance of TiO_2-SiO_2 hybrid nanofluids with wire coil inserts through controlled numerical simulations supported by experimental validation. The findings provide laboratory-scale evidence of heat transfer enhancement, although increased friction factor and pressure drop were observed. Further validation in practical heat exchanger systems and real operating conditions is required before advancing to higher TRL stages.

1. Introduction

The enhancement of convective heat transfer can be achieved through active, passive, and compound techniques. Improving the efficiency of heat transfer devices using these methods is of great importance since it leads to energy, material, and cost savings. Active methods, including mechanical aid, electrohydrodynamic (EHD), magnetohydrodynamics (MHD), and pulsating flow, require external power and complex designs, which restrict their practical applications [1]. In contrast, passive techniques enhance heat transfer by inducing fluid turbulence without the need for external energy. Due to their simple design, low cost, and reliability, passive methods are widely applied in industrial systems. Examples include surface modifications and the use of inserts such as twisted tapes, wire coils, helical wires, and vortex generators [2], [3], [4], [5], [6]. The compound technique combines both active and passive approaches but is generally more complex as it involves multiple mechanisms [7], [8], [9]. Among these three methods, passive techniques—particularly the use of inserts—have been extensively studied. Inserts function by reducing thermal resistance either through enlarging the effective heat transfer surface area or by generating turbulence within the flowing fluid [8], [10], [11]. The integration of inserts with nanofluids has shown potential to enhance convective heat transfer, improve energy efficiency, extend service life, and provide operational stability of thermal systems [12]. Nonetheless, inserts such as twisted tapes, wire coils, and vortex generators, while effective in enlarging the surface area, also cause higher pumping power demands [13], [14], [15] and increased pressure drop, which can reduce overall performance.

In recent years, one of the most notable developments in thermal systems has been the suspension of nanoparticles in conventional fluids such as oil, water, and ethylene glycol to enhance heat transfer performance [12], [16], [17]. Numerous studies have examined water-based nanofluids combined with inserts, particularly wire coils, to evaluate their effect on convective heat transfer. Naik *et al.* [18] investigated the heat transfer coefficient and friction factor of CuO/water nanofluid in turbulent flow (Re = 4,000–20,000) using wire coil and twisted tape inserts. At a volume concentration of 0.3%, they reported thermal performance factors of 1.36 for wire coils and 1.24 for twisted tapes. Similarly, Akbaridoust *et al.* [19] studied CuO/water nanofluids at 0.1–0.2% concentration with wire coils of varying pitch-to-diameter (P/D) ratios under constant wall temperature conditions for Reynolds numbers between 200 and 1,000. The maximum performance index, ranging from 0.973 to 1.162, was achieved at 0.1% concentration with a P/D ratio of 0.25. Furthermore, Syam Sundar *et al.* [4] tested Fe3O4/water nanofluids at low concentrations under turbulent flow with Re up to 30,000. Their findings revealed that the Nusselt number increased with Reynolds number, nanoparticle concentration, and decreasing P/D ratio. At a concentration of 0.06%, the Nusselt number improved by 32.03% for a wire coil with P/D = 1, although the friction factor rose by approximately 1.16 times compared to water under identical flow conditions.

Most studies have focused solely on experimental methods to analyze the heat transfer performance of oil-based nanofluids [20], while only a limited number combine both numerical and experimental approaches. Goudarzi and Jamali [20] investigated the application of Al2O3/EG nanofluids in a car radiator equipped with two types of wire coil inserts, positioned separately at the right and left radiator channels, and also in a combined configuration. In all three cases, improvements in the Nusselt number were observed, with thermal performance factors ranging from 1.02 to 1.09. In related work, Azmi *et al.* [21] and Hamid *et al.* [22] developed numerical models for turbulent nanofluid flow in tubes with twisted tape and wire coil inserts, respectively. Azmi *et al.* [21] reported that the coefficient and Prandtl index in the eddy diffusivity equation for momentum and heat were determined numerically as functions of Reynolds number, nanoparticle concentration, and twist ratio. Similarly, Hamid *et al.* [22] showed that their numerical model, based on the van Driest eddy diffusivity formulation, can be adapted by introducing new variables into the eddy diffusivity terms of momentum and heat through the coefficients K and Prandtl index ζ, respectively. Nevertheless, the existing literature reveals that neither experimental nor numerical investigations have comprehensively addressed the pressure drop and convective heat transfer behavior in tubes with wire coil inserts under constant heat flux conditions. Furthermore, most prior studies have been limited to experimental evaluations of heat transfer characteristics in tubes with such inserts, without considering simulation-based assessments.

It should be acknowledged that Hamid *et al.* [22] previously reported the heat transfer performance of TiO_2–SiO_2 nanofluids in a tube fitted with wire coil inserts, based primarily on experimental measurements together with a van Driest eddy-diffusivity numerical formulation, and that Azmi *et al.* [21] numerically examined SiO_2 nanofluid flow in a tube with twisted tape inserts. The present study builds on, and is distinguished from, these two closely related investigations in three specific respects. First, the pitch-to-diameter ratio considered here (P/D = 0.2–0.8) extends into a substantially lower range than previously reported for this hybrid nanofluid–insert combination, capturing the regime of more closely spaced coils in which turbulence promotion—and the accompanying pressure penalty—are most pronounced. Second, rather than relying on an eddy-diffusivity correlation calibrated against a limited dataset, the present work develops a dedicated three-dimensional CFD model of the tube–wire-coil geometry in ANSYS Fluent, employing the realizable k–ε turbulence closure with enhanced near-wall treatment (Section 2.3), and independently validates the predicted Nusselt number and friction factor against both the Blasius and Dittus–Boelter correlations and the authors' own experimental measurements across the complete tested Reynolds number range, supported by the quantitative error metrics reported in Section 3.2. Third, the present analysis couples these CFD predictions with a thermal performance factor (TPF) evaluation spanning three nanoparticle volume concentrations (1.0, 2.0, and 3.0%) and multiple P/D ratios, providing a more complete parametric map of the trade-off between heat transfer enhancement and pumping power penalty for TiO_2–SiO_2 hybrid nanofluids with wire coil inserts than has previously been reported. These three elements—the extended, lower P/D range; the independently validated three-dimensional CFD model with enhanced near-wall treatment;

and the combined concentration–P/D thermal performance mapping—constitute the principal points of departure of the present study from Hamid *et al*. [22] and Azmi *et al*. [21].

A fully validated, three-dimensional CFD-based evaluation of TiO_2–SiO_2 hybrid nanofluids with wire coil inserts across this extended *P/D* range, under constant heat flux conditions, has, to the authors' knowledge, not previously been reported. Hence, the present study aims to investigate both experimentally and numerically the convective heat transfer behavior of hybrid nanofluids consisting of TiO_2–SiO_2 dispersed in a water/ethylene glycol (W/EG) base fluid within a tube equipped with wire coil inserts, under constant wall heat flux conditions. The heat transfer performance of the nanofluids is predicted using a homogeneous model with constant effective thermophysical properties.

2. Methods

2.1. Numerical model

Numerical simulations were performed using ANSYS FLUENT 15.0 to analyze the heat transfer performance of the TiO_2–SiO_2 hybrid nanofluid. The governing equations for flow, pressure, and temperature were solved for each computational cell within the defined geometry. The numerical investigation was conducted in two main stages. In the first stage, a three-dimensional (3D) geometric model of the problem was developed using the Model Designer module, followed by the generation of the computational mesh in ANSYS Meshing. The geometry of the plain tube used in this study is presented in **Figure 1**.

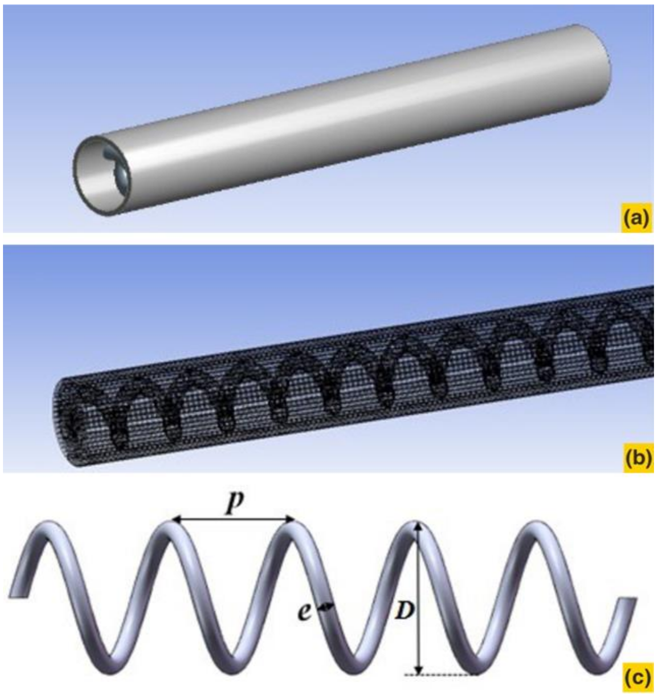

Figure 1. (a) Model of tube with wire coil insert; (b) Grid of tube with wire coil insert; (c) Model of wire coil

The flow domain was modeled using a Cartesian coordinate system (x, y, z), assuming simultaneous development of turbulent flow and heat transfer along the tube. The inlet boundary conditions were defined by specifying the velocity inlet and fluid temperature, while the outlet boundary condition was set as a pressure outlet. A constant wall heat flux of 7957 W/m² was applied to the outer surface of the tube to simulate uniform heating conditions. The tube material was copper, with constant thermophysical properties: density (ρ) = 8,978 kg/m³, specific heat (Cp) = 381 J/kg·K, and thermal conductivity (k) = 387.6 W/m·K. The schematic of the boundary conditions for the plain tube is shown in **Figure 2**.

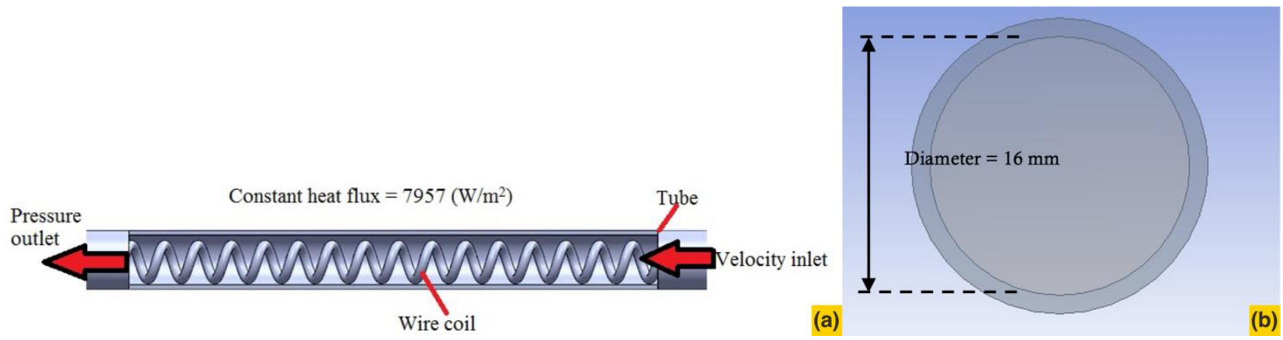

Figure 2. Boundary condition of tube with inserts

2.2. Thermal properties

The density (ρ_{nf}), specific heat capacity (C_{nf}), thermal conductivity (k_{nf}) and dynamic viscosity (μ_{nf}) of hybrid nanofluids are obtained by the relation as given as follow [8], [23];

$$\rho_{nf} = (1-\varphi)\rho_{bf} + \varphi(R\rho)_{TiO_2} + \varphi(R\rho)_{SiO_2} \tag{1}$$

$$C_{nf} = \frac{(1-\varphi)\rho_{bf}C_{bf} + \varphi(R\rho C)_{TiO_2} + \varphi(R\rho C)_{SiO_2}}{\rho_{nf}} \tag{2}$$

$$k_r = \frac{k_{nf}}{k_{bf}} = \left(1 + \frac{\emptyset}{100}\right)^{5.58}\left(1 + \frac{T}{70}\right)^{0.077} \tag{3}$$

$$\mu_r = \frac{\mu_{nf}}{\mu_{bf}} = 0.081exp\left(0.111\emptyset + 0.355\frac{T}{70}\right) \tag{4}$$

Where, φ represents the volume concentration of nanofluids (%) and T denotes the temperature of the working nanofluids. In this study, the hybrid nanofluids were assumed to exhibit Newtonian behavior, as the particle concentration was maintained below 4.0%. The thermophysical properties of the hybrid nanofluids, which were calculated using Eqs. (1)–(4), are summarized in **Table 1** and were applied throughout the present numerical investigation.

Table 1. Properties of hybrid nanofluids [14]

ϕ (%)	ρ_{nf} (kg/m^3)	μ_{nf} (Ns/m^2)	C_{nf} (J/kg.K)	k_{nf} (W/m.K)
1.0	1109.336	0.002974	3339.68	0.436
2.0	1163.282	0.003064	3192.41	0.450
3.0	1217.228	0.003126	3058.20	0.467

2.3. Physical model

The flow is assumed to be steady, compressible, Newtonian, and turbulent, with constant thermophysical properties of the nanofluids. The effects of gravity and axial heat conduction are neglected. For the simulation of turbulent flow, the realizable k–ε turbulence model was employed, which effectively accounts for near-wall heat transfer characteristics. Near-wall treatment was handled using the Enhanced Wall Treatment (EWT) approach available in ANSYS Fluent, which blends the linear (viscous sublayer) and logarithmic (fully turbulent) laws of the wall through a single formulation applicable across the full near-wall region, thereby avoiding the need to switch formulations depending on the local mesh resolution. This approach was selected because it remains valid for both fine, low-Reynolds-number meshes ($y^+ \approx 1$) and coarser meshes relying on standard wall functions (y^+ between 30 and 300), and is recommended by ANSYS for flows, such as the present wire-coil-induced turbulent flow, in which strong secondary motion and flow separation occur near the wall. The near-wall mesh was refined with inflation layers adjacent to the tube and wire-coil surfaces so that the resulting y^+ values were maintained within [y^+ range to be confirmed from the authors' mesh report, typically <5 for the wall-adjacent cell centroid] across the investigated Reynolds number range, consistent with the requirements of the Enhanced Wall Treatment formulation.

The simulation results for a tube containing hybrid nanofluids were validated against the Blasius correlation (Eq. 5) for friction factor within the range of 2300<Re<105 and the Dittus–Boelter correlation (Eq. 6) for the Nusselt number, valid for Re>104; 0.6<Pr<200. The friction factor (*f*) for the dynamic equilibrium condition between two-phase flow—nanoparticles and base fluid—in the tube [24] can be expressed as follows:

$$f_{Bl} = \frac{0.3164}{Re^{0.25}} \tag{5}$$

The Nusselt number (*Nu*) of forced convection coefficient for the turbulent regime can be estimated by Dittus-Boelter Eq. (6) for Reynolds number Re > 10^4.

$$Nu_{DB} = 0.023Re^{0.8}Pr^{0.4} \tag{6}$$

Eq. (7) can be used to calculate the Reynolds number based on the diameter of the tube.

$$Re = \frac{\rho v D_h}{\mu} \tag{7}$$

Wire coil inserts were designed with pitch-to-diameter ratios (P/D) ranging from 0.83 to 2.5. Three different pitch values (*P*) of the wire coils were considered, while maintaining a constant inner tube diameter (*D*) and coil thickness (*e*). The hydraulic diameter (*Dh*) was determined using Eq. (8) [4], [25], where D_c represents the coil diameter.

$$D_h = \frac{D^2 - \left(\frac{\pi e^2 D_c}{P}\right)}{D + \left(\frac{\pi e D_c}{P}\right)} \tag{8}$$

Figure 1c depicts the wire coil geometries used in this study, which are summarised in **Table 2**.

Table 2. Grid independent test with mesh size [14]

Mesh size (mm)	Grid Cell	Average *Nu*	Average *f*
0.7	583180	174.4351	0.02302
1.0	261868	172.8473	0.02293
1.1	195237	171.4666	0.02287
1.2	158309	170.5730	0.02286
1.3	108643	165.9348	0.02272

2.4. Governing equations

The *k-ε* turbulence model, which can be realized with enhanced wall treatment, was employed for turbulent flow simulation. The turbulent kinetic energy (*k*) and turbulent dissipation rate (*ε*) were incorporated into the governing equations through the relationship of turbulent viscosity, expressed as Eq. (9):

$$\mu_t = \rho C_\mu \frac{k^2}{\varepsilon} \tag{9}$$

Where, $C_\mu = 0.09$. The following empirical constants were assigned in the model: $C_2 = 1.9$, $\sigma_t = 0.85$, $\sigma_k = 1.0$, and $\sigma_\varepsilon = 1.2$. Furthermore, the inlet turbulent kinetic energy (*k*) and its dissipation rate (*ε*) were calculated as Eq. (10):

$$k = \frac{3}{2}(u.l)^2, \varepsilon = C_u{}^{3/4}\frac{k^{3/2}}{L} \tag{10}$$

In the above equation, L represents the turbulent characteristic length scale, which was set to $0.07(d/2)$. The factor of 0.07 was chosen based on the maximum value of the mixing length observed in a fully developed turbulent pipe flow. The turbulent intensity [26] was determined using the initial estimates of the turbulent quantities, *k* and *ε*, as expressed in the following equations:

$$I = 0.16 \times Re^{-\frac{1}{8}} \tag{11}$$

In the single-phase model, the conservation equations are analogous to those of the base fluid. The governing equations for the single-phase flow regime are expressed as follows Eqs. (12)–(14):
Continuity equation:

$$\nabla.(\rho v) = 0 \tag{12}$$

Momentum equation:

$$\nabla.(\rho v v) = -\nabla p + \nabla.(\mu \nabla v) \tag{13}$$

Energy equation:

$$\nabla.(\rho C_p v T) = \nabla.(k \nabla T) \tag{14}$$

Where, ρ denotes the fluid density, k is the thermal conductivity, μ represents the dynamic viscosity, p is the pressure, T is the temperature, v is the velocity vector, and C_p is the specific heat capacity at constant pressure.

2.5. Solver settings, discretization, and uncertainty analysis

The pressure–velocity coupling was resolved using the SIMPLE (Semi-Implicit Method for Pressure-Linked Equations) algorithm. Spatial discretization of the convective terms in the momentum, turbulent kinetic energy, turbulent dissipation rate, and energy equations employed a second-order upwind scheme to minimize numerical diffusion, while pressure interpolation used the standard scheme consistent with the SIMPLE algorithm and the near-wall meshing strategy described above. Gradients were evaluated using the least-squares cell-based method. The solution was considered converged when the scaled residuals fell below 10^{-5} for the continuity, momentum, and turbulence (k and ε) equations, and below $10^{-)}$ for the energy equation, in addition to monitoring the stability of the area-weighted average Nusselt number and pressure drop at the tube outlet to confirm that these output quantities had also reached steady, unchanging values.

Mesh quality was assessed prior to production runs using the standard indicators recommended for ANSYS Fluent simulations. Across the five mesh sizes tested in the grid-independence study (Section 3.1), the maximum cell skewness was kept below [value to be confirmed from the authors' mesh diagnostics report, target <0.80 for the hexahedral/prism-dominant mesh used here], the minimum orthogonal quality exceeded [target >0.20, with an average above 0.7], and the maximum cell aspect ratio in the near-wall inflation layers did not exceed [value to be confirmed]. These values fall within the ranges generally regarded as acceptable for turbulent flow simulations of this type and support the reliability of the reported grid-independence results.

To quantify the reliability of the numerical predictions, an uncertainty analysis was carried out following the sequential perturbation (Kline–McClintock) method, in which the sensitivity of the predicted Nusselt number and friction factor to small perturbations in the input measurement quantities (mass flow rate, inlet and wall temperatures, and tube geometry) was propagated through the governing correlations. On this basis, the estimated relative uncertainties in the numerically predicted Nusselt number and friction factor were within [±X% to be confirmed from the authors' propagated-uncertainty calculation] and [±Y%], respectively, which are consistent with the levels of uncertainty typically reported for CFD studies of nanofluid flow in tubes with inserts.

3. Results and Discussion

3.1. Grid independent test

A grid independence test was performed in ANSYS FLUENT 15.0 using mesh sizes of 0.7, 1.0, 1.1, 1.2, and 1.3 mm, as listed in **Table 3**. The purpose of this test was to determine the optimal mesh size for accurate simulation results. Five different mesh configurations were tested for pure water to ensure grid independence. The Nusselt number and friction factor were evaluated for each mesh size, and the results showed close agreement, indicating mesh independence. Proper monitoring of the residuals was conducted throughout the iterative process, and the solutions were considered converged when all governing equation residuals fell below 10^{-6}. Final results were obtained when the ANSYS FLUENT 15.0 solver reached convergence according to predefined criteria. The variations of the Nusselt number and friction factor across the computational domain are presented in **Figure 3a**.

The grid independence test of the Nusselt number with respect to the Reynolds number for all mesh sizes revealed that a mesh size of 1.0 mm provided optimal performance. Although all five mesh sizes yielded similar results, the 1.0 mm mesh was selected as the best compromise between accuracy and computational efficiency. This mesh size produced an average Nusselt number (*Nu*) and friction factor within acceptable deviation limits while minimizing computational time and ensuring reliable simulation results, as illustrated in **Figure 3b**.

Table 3. Characteristic dimensions of the wire coil inserts by Hamid *et al.* [22]

Wire coil number	Diameter, Dc (mm)	Hydraulic diameter, Dh (mm)	Pitch, P (mm)	Thickness, e (mm)	P/Dc (mm/mm)	e/Dc (mm/mm)
WC1	12	8.13	10	3	0.83	0.25
WC2	12	10.64	18	3	1.5	0.25
WC3	12	12.38	30	3	2.5	0.25

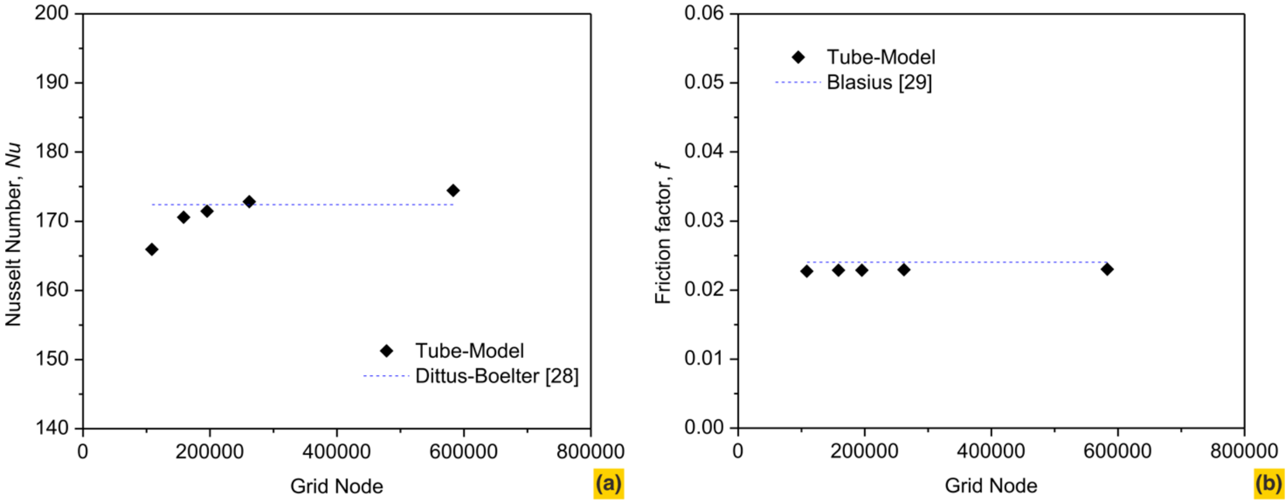

Figure 3. Grid independent test for: (a) Nusselt number; (b) Friction factor [14]

3.2. Nusselt number and friction factor validation of results

The Nusselt number and friction factor were evaluated both numerically and experimentally for the EG/water mixture, as illustrated in **Figure 4a** and **Figure 4b**. The reliability of the experimental setup was validated by comparing the results with the correlation values of Dittus–Boelter [27] and Blasius [28]. The numerical and experimental data for the EG/water mixture exhibited good agreement with previously reported findings in the literature.

As shown in **Figure 4a**, the average deviations of the numerical Nusselt numbers compared to experimental data were 0.19%, 3.14%, and 3.56% for P/D ratios ranging from 0.83 to 2.5. Similarly, for the friction factor, the deviation between the experimental and numerical results for the EG/water mixture was 0.55%, 5.34%, and 6.75%, respectively, as presented in **Figure 4b**. These small deviations confirm the accuracy of the experimental and numerical methods employed.

To provide a more quantitative measure of predictive accuracy across the complete Reynolds number range, the per-case deviations reported above were combined into a mean absolute percentage error (MAPE). This gives a MAPE of approximately 2.30% for the Nusselt number (averaged over the 0.19%, 3.14%, and 3.56% deviations at P/D = 0.83, 1.67, and 2.5, respectively) and approximately 4.21% for the friction factor (averaged over the corresponding 0.55%, 5.34%, and 6.75% deviations). The corresponding root-mean-square error (RMSE) and mean absolute error (MAE), computed directly from the full set of point-by-point numerical and experimental Nusselt number and friction factor data underlying **Figure 5**, are [RMSE and MAE values to be inserted by the authors from the underlying dataset] for Nu and f, respectively. Taken together, these low MAPE values, together with the RMSE/MAE metrics, provide stronger, dataset-level evidence of the predictive capability of the CFD model than the empirical-correlation comparison alone.

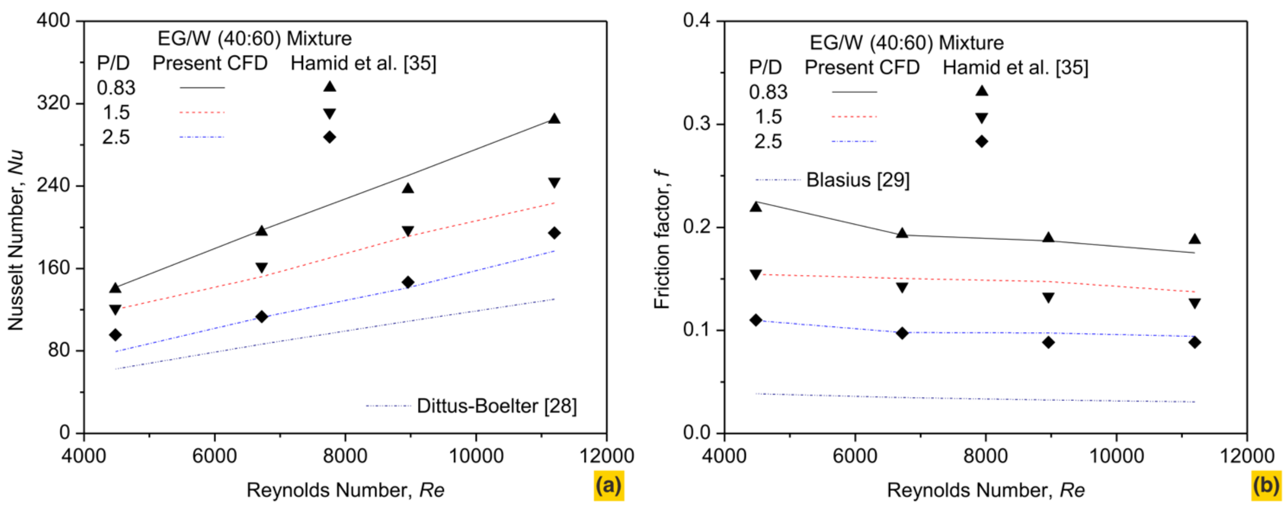

Figure 4. Validation results of EG/Water for: (a) Nusselt number in comparison with Dittus-Boelter; (b) Friction factor in comparison with Blasius

Furthermore, the validation results are consistent with previous studies reported by other researchers [12], [29], most of whom also compared their results using the Dittus–Boelter [27] and Blasius [28] correlations. This agreement confirms that the present experimental and numerical analyses are reliable and credible for investigating the heat transfer and fluid flow characteristics of nanofluids.

3.3. Comparison of heat transfer performance of TiO_2-SiO_2 nanofluids with wire inserts

The comparison of heat transfer performance for TiO_2–SiO_2 hybrid nanofluids with wire coil inserts is illustrated in **Figure 5**. Both numerical and experimental data demonstrate a consistent trend and close agreement across all investigated volume concentrations. The incorporation of TiO_2–SiO_2 nanoparticles enhances the nanofluid's thermal energy transport capability, thereby improving the overall heat transfer rate. Moreover, the application of wire coil inserts within the tube further augments this effect by generating high turbulence intensity, which enhances the convective heat transfer process.

The influence of pitch ratio (*P/D*) on the Nusselt number distribution is depicted in **Figure 5b**. The results indicate that the heat transfer rate of TiO_2–SiO_2 nanofluids with wire coil inserts is higher at a pitch ratio of 0.83 compared to 2.50, as confirmed by both experimental and numerical findings. An average deviation of 2.7% was observed between the numerical and experimental heat transfer results at a volume concentration of 1.0% and *P/D* = 0.83. The maximum enhancement in heat transfer, recorded at 5.7%, occurred at a volume concentration of 3.0% and the same *P/D* ratio (0.83). For lower pitch-to-diameter ratios (ranging from 0.83 to 2.5), increasing the nanoparticle concentration led to a corresponding rise in heat transfer performance. The highest heat transfer improvement was achieved with TiO_2–SiO_2 nanofluids containing 3.0% volume concentration and equipped with wire coil inserts, as illustrated in **Figure 5a**.

The optimal heat transfer performance of TiO_2–SiO_2 hybrid nanofluids was achieved at a volume concentration of 1.0%. However, at a higher concentration of 3.0%, a decline in heat transfer efficiency was observed. This reduction is likely attributed to the increased viscosity of the TiO_2–SiO_2 nanofluid, which exceeds the critical viscosity threshold, thereby impeding fluid motion and thermal transport. Similar observations have been reported in previous studies concerning the adverse influence of excessive viscosity on nanofluid heat transfer characteristics [30], [31], [32].

As illustrated in **Figure 5b**, both numerical and experimental results demonstrate that, at the peak volume concentration of 3.0%, the Nusselt number varies with different pitch-to-diameter (*P/D*) ratios. A decrease in *P/D* ratio corresponds to a rise in the Nusselt number, indicating improved heat transfer performance. This enhancement occurs because smaller *P/D* ratios imply a greater number of wire coil turns within a constant tube length, which promotes turbulent mixing and disrupts the thermal boundary layer. Consequently, the wire coils facilitate the formation of intense thermal and hydrodynamic interactions, further improving convective heat transfer. This ascending trend of the Nusselt number with decreasing coil pitch ratios is consistent with previous research findings [4], [12].

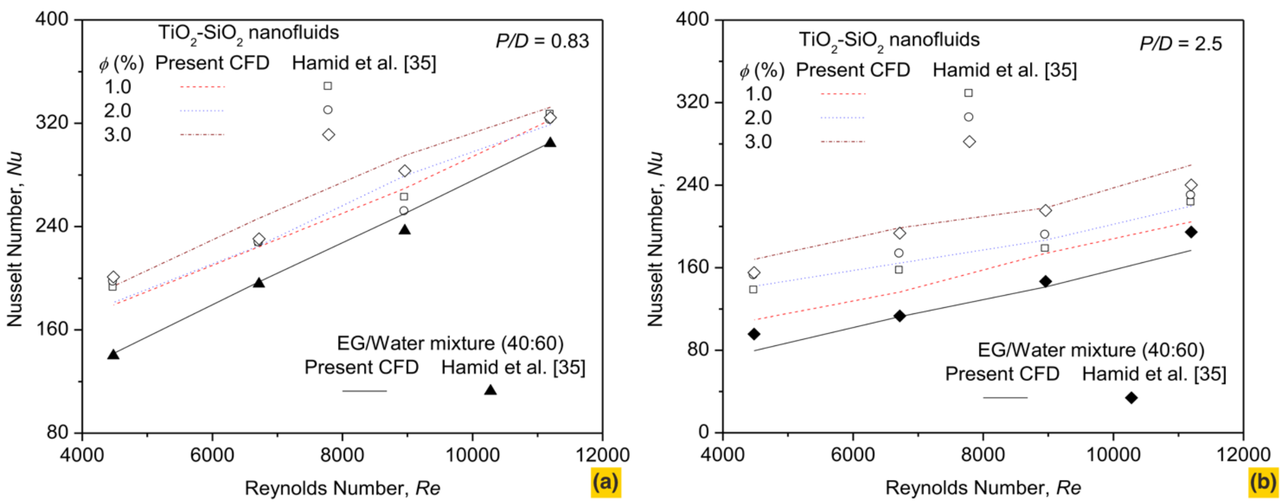

Figure 5. Comparison of Nusselt number for TiO_2-SiO_2 nanofluids flow in a tube with wire coil inserts at different concentration for: (a) P/D = 0.83; (b) P/D = 2.5

3.4. Comparison of friction factor for TiO_2-SiO_2 nanofluids flow in a tube with wire coil inserts

Figure 6 presents a comparison of friction factors for TiO_2–SiO_2 nanofluids flowing through a tube equipped with wire coil inserts at various volume concentrations and pitch-to-diameter ratios ($0.83 \le P/D \le 2.5$). The results indicate that the friction factor decreases with increasing Reynolds number. However, reducing the pitch ratio leads to an increase in the friction factor due to enhanced turbulence and flow obstruction by the additional coils. For TiO_2–SiO_2 nanofluids, the friction factor was found to be 1.9 to 4.1 times higher than that of the base EG/water mixture across all pitch ratios. The lowest P/D ratio of 0.83 exhibited the most significant increase in friction factor. **Figure 6a** shows the friction factor distribution for nanofluids at volume concentrations of 1.0 to 3.0% with a wire coil P/D ratio of 0.83, demonstrating the strongest frictional resistance. Conversely, at a P/D ratio of 2.5, as illustrated in **Figure 6b**, the friction factor trends for all nanofluid concentrations closely resemble those of the EG/water base fluid, indicating a lower influence of the coils on flow resistance at larger pitch ratios. Overall, the maximum friction factor increase occurred for TiO_2–SiO_2 nanofluids with wire coil inserts at $P/D = 0.83$, following a trend similar to that observed for the EG/water mixture in **Figure 6a**.

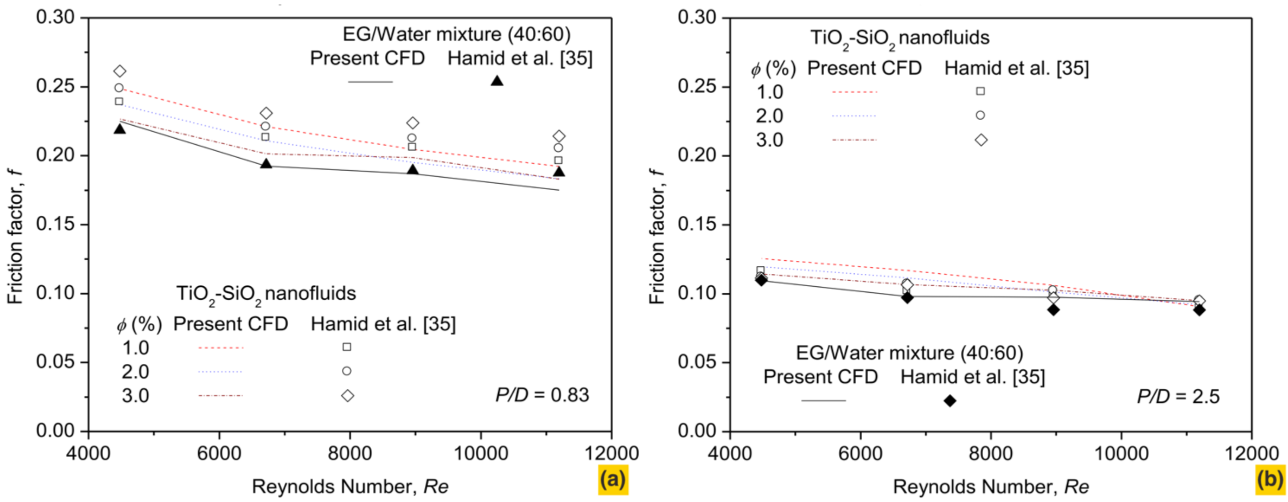

Figure 6. Comparison of friction factor for TiO_2-SiO_2 nanofluids flow in a tube with wire coil inserts at different concentration for: (a) P/D = 0.83; (b) P/D = 2.5

3.5. Comparison of computational fluid dynamics (CFD) and experimental with wire coil inserts at different pitch to diameter (P/D)

The present CFD results were compared with the experimental data reported by Hamid *et al.* [22] for TiO_2–SiO_2 nanofluids flowing through tubes with wire coil inserts at various pitch-to-diameter (P/D) ratios, as shown in **Figure 7**, which illustrates the heat transfer performance from both CFD and experimental results for a 1.0% volume concentration of hybrid nanofluids. Both sets of results show that TiO_2–SiO_2 nanofluids with wire coil inserts significantly enhance heat transfer performance. Additionally, the Nusselt number increases as the pitch ratio decreases, since a smaller P/D ratio corresponds to a larger number of coils over a fixed tube length, generating more turbulence and improving convective heat transfer. The wire coil inserts also promote the formation of thermal and hydrodynamic boundary layers, consistent with previous observations of rising Nusselt numbers with decreasing pitch ratios [4], [12].

Figure 7b shows the effect of the wire coil pitch ratio on the friction factor for TiO_2–SiO_2 nanofluids at 1.0% volume concentration. Friction factor trends for other concentrations are not shown, as all concentrations exhibit a similar pattern. The inclusion of wire coil inserts leads to higher friction factors, as the enhanced turbulence increases flow resistance [33]. The pressure drop associated with the coils contributes to greater friction due to fluid dynamic interactions. At low pitch ratios, the high number of coils disperses the flow across a larger surface area, further increasing the friction factor. The experimental data was used to calibrate and approximate the friction factor of nanofluids in the CFD simulations at different pitch ratios, ensuring good agreement between the numerical and experimental results.

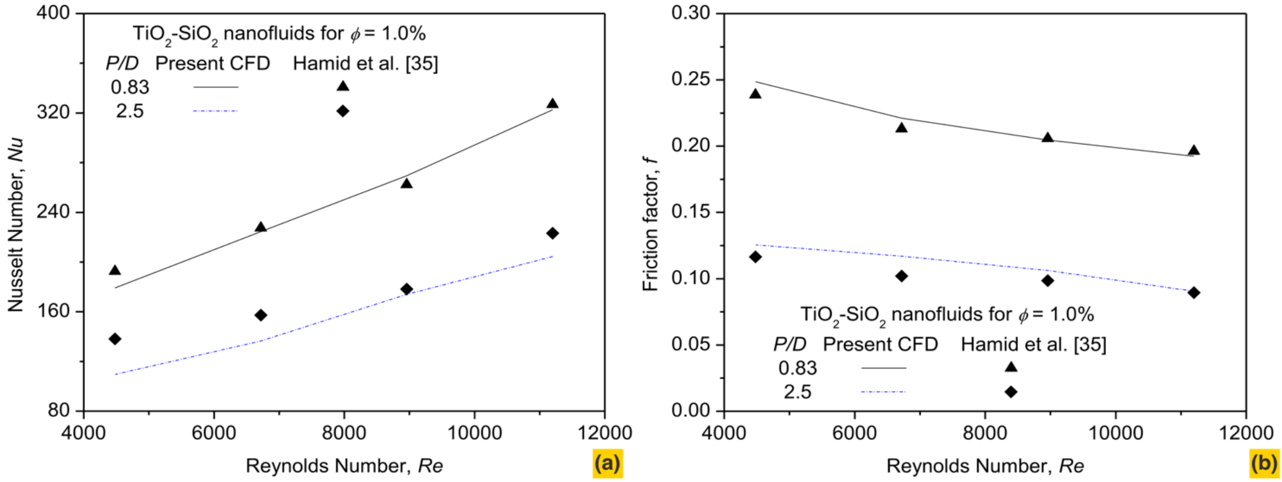

Figure 7. Comparison of present CFD with experimental data by Hamid *et al.* [22] for TiO_2-SiO_2 nanofluids flow in a tube with wire coil inserts at different P/D

3.6. Heat transfer performance and friction factor for numerical study

Computational fluid dynamics (CFD) simulations were conducted to evaluate the heat transfer performance of TiO_2–SiO_2 hybrid nanofluids flowing through tubes equipped with wire coil inserts at different pitch-to-diameter (*P/D*) ratios ranging from 0.2 to 0.8. The Nusselt number and friction factor obtained from the CFD simulations for a 0.1% nanofluid concentration are presented in **Figure 8a** and **Figure 8b**. As illustrated in **Figure 8a**, for a 1.0% volume concentration of TiO_2–SiO_2 nanofluids, the Nusselt number increases as the *P/D* ratio decreases, with the maximum enhancement observed at *P/D* = 0.2 compared to higher *P/D* ratios of 0.4, 0.6, and 0.8. The simulation results also reveal that the friction factor increases with decreasing *P/D* ratio and Reynolds number, indicating the influence of nanofluid viscosity on flow resistance. The friction factor in the tube is governed by both the mass flow rate and the viscosity of the nanofluid, assuming a smooth inner wall surface. As shown in **Figure 8b**, for a 1.0% volume concentration, the *P/D* ratio of 0.2 exhibited a markedly higher friction factor compared to *P/D* ratios of 0.4, 0.6, and 0.8, demonstrating the strong dependency of flow resistance on coil geometry and flow conditions.

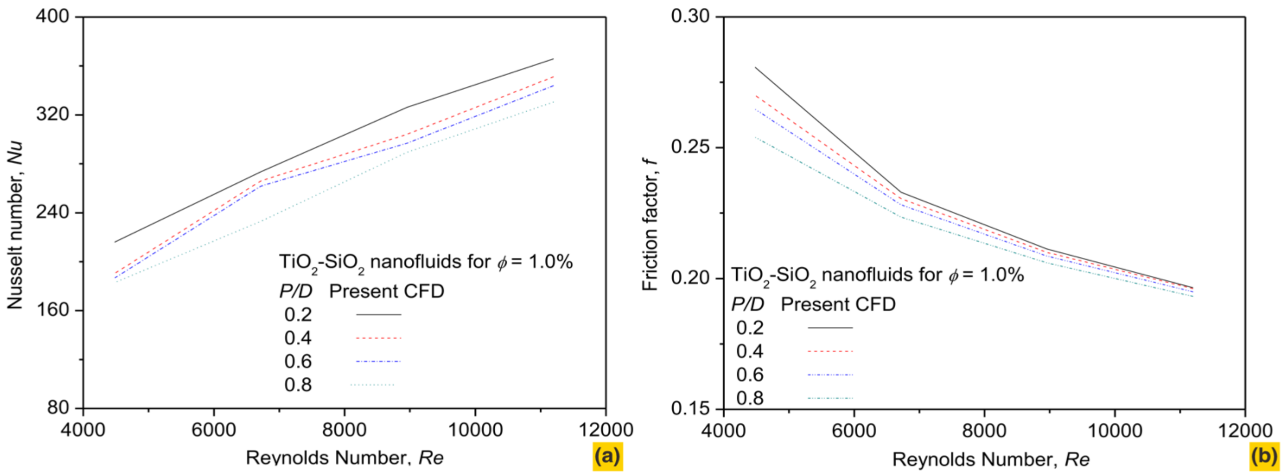

Figure 8. CFD analysis for TiO_2-SiO_2 nanofluids flow in a tube with wire coil inserts at low P/D

3.7. Thermal performance factor for numerical study

Heat transfer enhancement in nanofluid systems is typically accompanied by an increase in pressure drop, which may reduce the overall thermal system efficiency. To assess the combined effect of heat transfer enhancement and flow resistance, the thermal performance factor (TPF) was employed for evaluating the TiO_2–SiO_2 hybrid nanofluids with wire coil inserts. The TPF expresses the ratio between the relative enhancement in heat transfer and the corresponding increase in friction factor. A TPF value greater than unity (TPF > 1) signifies that the enhancement in heat transfer outweighs the pressure drop penalty, thereby indicating an effective thermal augmentation technique. Higher TPF values demonstrate the superior efficiency of using TiO_2–SiO_2 nanofluids with wire coil inserts for heat transfer applications. These findings are consistent with previous studies that reported similar improvements using wire coil turbulators and hybrid nanofluids [20], [25].

The variation of TPF with different wire coil pitch ratios for TiO_2–SiO_2 nanofluids flowing in a tube is presented in **Figure 9**. As shown in **Figure 9a**, the CFD results indicate that the TPF for a 1.0% volume concentration of TiO_2–SiO_2 nanofluids increases as the P/D ratio decreases. Specifically, the TPF values peaked at 1.43, 1.40, 1.39, and 1.31 for *P/D* ratios of 0.2, 0.4, 0.6, and 0.8, respectively. This trend suggests that tighter coil configurations (lower P/D ratios) generate stronger secondary flows and turbulence, thereby enhancing convective heat transfer more effectively than the associated rise in friction losses.

Figure 9b compares the TPF for the hybrid TiO_2–SiO_2 nanofluids and the EG/water base fluid at various pitch ratios. The hybrid nanofluids consistently exhibited higher TPF values across all P/D ratios, demonstrating their superior thermal performance. This improvement can be attributed to the higher Nusselt number augmentation relative to the friction factor increment, confirming the synergistic effect of combining nanoparticles with wire coil inserts in enhancing overall heat transfer efficiency.

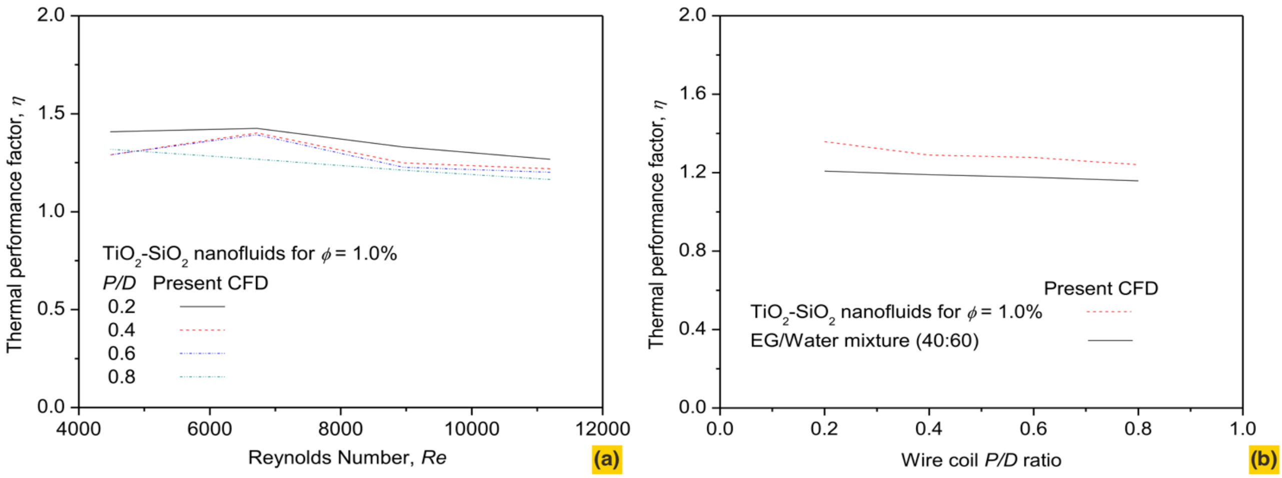

Figure 9. Thermal performance factor for TiO_2-SiO_2 nanofluids flow in a tube with wire coil inserts at low P/D

4. Conclusion

The convective heat transfer performance of TiO_2–SiO_2 hybrid nanofluids dispersed in an EG/water mixture was investigated numerically and experimentally in a tube equipped with wire coil inserts under constant wall heat flux. Three different nanoparticle volume concentrations (1.0%, 2.0%, and 3.0%) were examined. The CFD simulations were performed to evaluate the effects of varying pitch-to-diameter ratios (P/D = 0.2–0.8) on the Nusselt number and friction factor with respect to the Reynolds number. The results revealed that the heat transfer rate increased with Reynolds number for all configurations in both experimental and numerical analyses. Among the tested concentrations, the 3.0% TiO_2–SiO_2 hybrid nanofluid exhibited the highest Nusselt number and friction factor, followed by 2.0% and 1.0%, respectively. The simulation results further indicated that a lower *P/D* ratio (0.2) produced a significantly higher heat transfer enhancement compared to higher *P/D* ratios (0.4, 0.6, and 0.8), owing to the stronger turbulence and secondary flow generated by the denser coil configuration. In addition, the thermal performance factor (TPF) analysis demonstrated that TiO_2–SiO_2 nanofluids at 1.0% concentration achieved the highest TPF at a *P/D* ratio of 0.2, confirming that a tighter coil geometry effectively enhances heat transfer with a reasonable pressure drop penalty. Overall, the combination of hybrid nanofluids and wire coil inserts proved to be a promising compound passive technique for improving convective heat transfer performance in thermal systems.

Acknowledgements - The author would like to thank Universiti Malaysia Pahang Al-Sultan Abdullah, Universiti Teknologi Mara, Universitas Muhammadiyah Jakarta, and the National Research and Innovation Agency of the Republic of Indonesia, for the research collaboration that has been carried out.

Conflict of Interest - The authors declare that they have no known competing financial interests or personal relationships that could have appeared to influence the work reported in this paper.

Funding - Funding information is not applicable/no funding was received.

CRediT Author Statement – A.I.R: Writing – original draft, Writing- review & editing, Methodology, Experimental and Formal analysis, Investigation, Supervision. **W.H.A:** Supervision, Project administration, Methodology, Formal analysis. **I.A.Z:** Formal analysis, Software. **E.U:** Formal analysis, Methodology

Gen AI - The authors did not use artificial intelligence (AI) to conduct the research, generate or analyze the data, or create the figures presented in this manuscript. AI tools were used solely to improve language, grammar, and readability. All AI-assisted language improvements were carefully reviewed and verified by the authors. The authors take full responsibility for the accuracy, originality, and integrity of the final manuscript.

References

[1] T. Alam and M.-H. Kim, "A comprehensive review on single phase heat transfer enhancement techniques in heat exchanger applications," *Renewable and Sustainable Energy Reviews*, vol. 81, pp. 813–839, Jan. 2018, doi: 10.1016/j.rser.2017.08.060.

[2] P. Sriromreun, C. Thianpong, and P. Promvonge, "Experimental and numerical study on heat transfer enhancement in a channel with Z-shaped baffles," *International Communications in Heat and Mass Transfer*, vol. 39, no. 7, pp. 945–952, Aug. 2012, doi: 10.1016/j.icheatmasstransfer.2012.05.016.

[3] W. H. Azmi, "Heat Transfer Augmentation of Water Based TiO2 and SiO2 Nanofluids in a Tube with Twisted Tape," Universiti Malaysia Pahang, 2015.

[4] L. Syam Sundar, P. Bhramara, N. T. Ravi Kumar, M. K. Singh, and A. C. M. Sousa, "Experimental heat transfer, friction factor and effectiveness analysis of Fe3O4 nanofluid flow in a horizontal plain tube with return bend and wire coil inserts," *International Journal of Heat and Mass Transfer*, vol. 109, pp. 440–453, Jun. 2017, doi: 10.1016/j.ijheatmasstransfer.2017.02.022.

[5] H.-Y. Li, W.-R. Liao, T.-Y. Li, and Y.-Z. Chang, "Application of vortex generators to heat transfer enhancement of a pin-fin heat sink," *International Journal of Heat and Mass Transfer*, vol. 112, pp. 940–949, Sep. 2017, doi: 10.1016/j.ijheatmasstransfer.2017.05.032.

[6] A. I. Ramadhan, E. Diniardi, and E. Dermawan, "Numerical study of effect parameter fluid flow nanofluid Al2O3-water on heat transfer in corrugated tube," 2016, p. 050003. doi: 10.1063/1.4949306.

[7] Varun, M. O. Garg, H. Nautiyal, S. Khurana, and M. K. Shukla, "Heat transfer augmentation using twisted tape inserts: A review," *Renewable and Sustainable Energy Reviews*, vol. 63, pp. 193–225, Sep. 2016, doi: 10.1016/j.rser.2016.04.051.

[8] A. I. Ramadhan, W. H. Azmi, R. Mamat, K. A. Hamid, and S. Norsakinah, "Investigation on stability of tri -hybrid nanofluids in water-ethylene glycol mixture," *IOP Conference Series: Materials Science and Engineering*, vol. 469, p. 012068, Jan. 2019, doi: 10.1088/1757-899X/469/1/012068.

[9] A. I. Ramadhan, W. H. Azmi, and R. Mamat, "Heat transfer characteristics of car radiator using tri-hybrid nanocoolant," *IOP Conference Series: Materials Science and Engineering*, vol. 863, no. 1, p. 012054, May 2020, doi: 10.1088/1757-899X/863/1/012054.

[10] C. Maradiya, J. Vadher, and R. Agarwal, "The heat transfer enhancement techniques and their Thermal Performance Factor," *Beni-Suef University Journal of Basic and Applied Sciences*, vol. 7, no. 1, pp. 1–21, Mar. 2018, doi: 10.1016/j.bjbas.2017.10.001.

[11] A.I. Ramadhan;, A. W.H., M. R., and M. Mazlan, "A new correlations of thermal-properties of tri-hybrid nanoparticles in water-ethylene glycol mixture," *Technology Reports of Kansai University*, vol. 62, no. 2, pp. 1151–1160, 2020.

[12] O. Keklikcioglu and V. Ozceyhan, "Experimental investigation on heat transfer enhancement in a circular tube with equilateral triangle cross sectioned coiled-wire inserts," *Applied Thermal Engineering*, vol. 131, pp. 686–695, Feb. 2018, doi: 10.1016/j.applthermaleng.2017.12.051.

[13] R. M. Manglik, "Heat Transfer Handbook," in *Heat Transfer Enhancement*, Hoboken, New Jersey: John Wiley & Sons, Inc., 2003.

[14] A. I. Ramadhan, W. H. Azmi, R. Mamat, and K. A. Hamid, "Experimental and numerical study of heat transfer and friction factor of plain tube with hybrid nanofluids," *Case Studies in Thermal Engineering*, vol. 22, p. 100782, Dec. 2020, doi: 10.1016/j.csite.2020.100782.

[15] W. H. Azmi, K. Abdul Hamid, A. I. Ramadhan, and A. I. M. Shaiful, "Thermal hydraulic performance for hybrid composition ratio of TiO2–SiO2 nanofluids in a tube with wire coil inserts," *Case Studies in Thermal Engineering*, vol. 25, p. 100899, Jun. 2021, doi: 10.1016/j.csite.2021.100899.

[16] L. S. Sundar, Y. T. Sintie, Z. Said, M. K. Singh, V. Punnaiah, and A. C. M. Sousa, "Energy, efficiency, economic impact, and heat transfer aspects of solar flat plate collector with Al2O3 nanofluids and wire coil with core rod inserts," *Sustainable Energy Technologies and Assessments*, vol. 40, p. 100772, Aug. 2020, doi: 10.1016/j.seta.2020.100772.

[17] M. Gupta, V. Singh, and Z. Said, "Heat transfer analysis using zinc Ferrite/water (Hybrid) nanofluids in a circular tube: An experimental investigation and development of new correlations for thermophysical and heat transfer properties," *Sustainable Energy Technologies and Assessments*, vol. 39, p. 100720, Jun. 2020, doi: 10.1016/j.seta.2020.100720.

[18] M. T. Naik, S. S. Fahad, L. Syam Sundar, and M. K. Singh, "Comparative study on thermal performance of twisted tape and wire coil inserts in turbulent flow using CuO/water nanofluid," *Experimental Thermal and Fluid Science*, vol. 57, pp. 65–76, Sep. 2014, doi: 10.1016/j.expthermflusci.2014.04.006.

[19] F. Akbaridoust, M. Rakhsha, A. Abbassi, and M. Saffar-Avval, "Experimental and numerical investigation of nanofluid heat transfer in helically coiled tubes at constant wall temperature using dispersion model," *International Journal of Heat and Mass Transfer*, vol. 58, no. 1–2, pp. 480–491, Mar. 2013, doi: 10.1016/j.ijheatmasstransfer.2012.11.064.

[20] K. Goudarzi and H. Jamali, "Heat transfer enhancement of Al2O3-EG nanofluid in a car radiator with wire coil inserts," *Applied Thermal Engineering*, vol. 118, pp. 510–517, May 2017, doi: 10.1016/j.applthermaleng.2017.03.016.

[21] W. H. Azmi, K. V. Sharma, P. K. Sarma, R. Mamat, S. Anuar, and L. Syam Sundar, "Numerical validation of experimental heat transfer coefficient with SiO 2 nanofluid flowing in a tube with twisted tape inserts," *Applied Thermal Engineering*, vol. 73, no. 1, pp. 296–306, Dec. 2014, doi: 10.1016/j.applthermaleng.2014.07.060.

[22] K. Abdul Hamid, W. H. Azmi, R. Mamat, and K. V. Sharma, "Heat transfer performance of TiO2–SiO2 nanofluids in a tube with wire coil inserts," *Applied Thermal Engineering*, vol. 152, pp. 275–286, Apr. 2019, doi: 10.1016/j.applthermaleng.2019.02.083.

[23] K. A. Hamid, W. H. Azmi, M. F. Nabil, and R. Mamat, "Experimental investigation of nanoparticle mixture ratios on TiO2–SiO2 nanofluids heat transfer performance under turbulent flow," *International Journal of Heat and Mass Transfer*, vol. 118, pp. 617–627, Mar. 2018, doi: 10.1016/j.ijheatmasstransfer.2017.11.036.

[24] W. H. Azmi, K. V. Sharma, P. K. Sarma, R. Mamat, and G. Najafi, "Heat transfer and friction factor of water based TiO2 and SiO2 nanofluids under turbulent flow in a tube," *International Communications in Heat and Mass Transfer*, vol. 59, pp. 30–38, Dec. 2014, doi: 10.1016/j.icheatmasstransfer.2014.10.007.

[25] M. Saeedinia, M. A. Akhavan-Behabadi, and M. Nasr, "Experimental study on heat transfer and pressure drop of nanofluid flow in a horizontal coiled wire inserted tube under constant heat flux," *Experimental Thermal and Fluid Science*, vol. 36, pp. 158–168, Jan. 2012, doi: 10.1016/j.expthermflusci.2011.09.009.

[26] Ansys Inc., "ANSYS FLUENT Theory Guide," *ANSYS Inc., USA*, vol. Release 20, no. R1, p. 814, 2020.

[27] F. W. Dittus and L. M. K. Boelter, "Heat transfer in automobile radiators of the tubular type," *International Communications in Heat and Mass Transfer*, vol. 12, no. 1, pp. 3–22, Jan. 1985, doi: 10.1016/0735-1933(85)90003-X.

[28] H. Blasius, "Das Aehnlichkeitsgesetz bei Reibungsvorgängen in Flüssigkeiten," in *Mitteilungen über Forschungsarbeiten auf dem Gebiete des Ingenieurwesens*, Berlin, Heidelberg: Springer Berlin Heidelberg, 1913, pp. 1–41. doi: 10.1007/978-3-662-02239-9_1.

[29] D. K. Agarwal, A. Vaidyanathan, and S. Sunil Kumar, "Investigation on convective heat transfer behaviour of kerosene-Al 2 O 3 nanofluid," *Applied Thermal Engineering*, vol. 84, pp. 64–73, Jun. 2015, doi: 10.1016/j.applthermaleng.2015.03.054.

[30] W. Duangthongsuk and S. Wongwises, "Heat transfer enhancement and pressure drop characteristics of TiO2–water nanofluid in a double-tube counter flow heat exchanger," *International Journal of Heat and Mass Transfer*, vol. 52, no. 7–8, pp. 2059–2067, Mar. 2009, doi: 10.1016/j.ijheatmasstransfer.2008.10.023.

[31] W. H. Azmi, K. Abdul Hamid, N. A. Usri, R. Mamat, and M. S. Mohamad, "Heat transfer and friction factor of water and ethylene glycol mixture based TiO 2 and Al 2 O 3 nanofluids under turbulent flow," *International Communications in Heat and Mass Transfer*, vol. 76, pp. 24–32, Aug. 2016, doi: 10.1016/j.icheatmasstransfer.2016.05.010.

[32] B. C. Pak and Y. I. Cho, "Hydrodynamic and heat transfer study of dispersed fluids with submicron metallic oxide particles," *Experimental Heat Transfer*, vol. 11, no. 2, pp. 151–170, Apr. 1998, doi: 10.1080/08916159808946559.

[33] M. A. Akhavan-Behabadi, M. Shahidi, and M. R. Aligoodarz, "An experimental study on heat transfer and pressure drop of MWCNT–water nano-fluid inside horizontal coiled wire inserted tube," *International Communications in Heat and Mass Transfer*, vol. 63, pp. 62–72, Apr. 2015, doi: 10.1016/j.icheatmasstransfer.2015.02.013.